APPLICATION OF A FULL POTENTIAL METHOD TO PRACTICAL PROBLEMS IN SUPERSONIC AIRCRAFT DESIGN AND ANALYSIS*

K. B. Walkley and G. E. Smith
DEI-Tech, Inc.
Newport News, Virginia

Abstract

A method based on the conservation form of the full potential equation has been used to analyze realistic aircraft configurations at supersonic speeds. A fighter forebody with and without a canopy and a supersonic cruise wing-body concept have been addressed in the Mach 1.41 to 2.30 speed range. Comparisons of predicted and measured surface pressure distributions and lift and drag for the forebody configurations showed excellent to good correlations although some oscillations in the computed pressures were observed. Good to excellent results for the wing-body configuration were obtained as well. The nonlinear behavior of the pitching moment was well predicted although the magnitudes were somewhat low. These analyses have all been conducted using single-precision arithmetic on a VAX 11/780 computer. Execution times averaged from one-half to three quarters of an hour for the forebody configurations and slightly over four hours for the wing-body.

Nomenclature

C_D	Drag coefficient
C_L	Lift coefficient
C_P	Pressure coefficient
CPU	Central processing unit
C_m	Pitching moment coefficient
l	Length
M_∞	Freestream Mach number
x,y,z	Cartesian coordinates
α	Angle of attack
γ	Ratio of specific heats
ξ,η	Curvilinear coordinates in circumferential and normal directions
Φ	Velocity potential

Subscripts:

b	Body
c	Canopy
FRIC	Skin friction
PL	Canopy-forebody parting line
TCL	Forebody top centerline

Introduction

Linear theory methods[1] have been widely used for many years in the aerodynamic design and analysis of slender supersonic configurations[2,3]. The application of these methods is relatively straightforward and the required computer resources are modest. As the design flight envelope of advanced fighter aircraft expands to include both efficient supersonic cruise and supersonic maneuver requirements, the linear theory methods become increasingly inappropriate tools for the aircraft designer. To more accurately estimate the aerodynamics of such vehicles, the designer must look to the nonlinear aerodynamic methodologies.

The nonlinear methodologies include methods based on the Navier-Stokes, Euler, and full potential equations. Due to computer limitations, the application of the full Navier-Stokes equations to arbitrary and complex geometries is not yet a practical reality, but significant progress has been made using the thin layer approximation.[4] Euler solvers also require substantial computer resources and are somewhat restricted in the

* This work was supported by the United States Air Force, Aeronautical Systems Division/XRH, WPAFB, Ohio

complexity of configurations which can be analyzed.[5] Impressive advances are being made, however, in the application of the Euler equations to practical problems in aircraft design[6], and combinations of Euler and linear theory methods have proven useful for designing a fighter aircraft wing.[7]

Techniques based on the full potential equation offer a very attractive alternative to the Euler equations approach. The full potential techniques are capable of providing results which are equivalent to the Euler results when the assumptions of irrotational and isentropic flow are valid. A significant reduction in computer resources also occurs when the full potential method is selected.

The purpose of this paper is to present and discuss the results of several analyses conducted using a full potential method[8]. Both pressure coefficient and force and moment coefficient comparisons with test results for several cases are included at supersonic Mach numbers ranging from 1.41 to 2.30. Practical problems such as determining forebody aerodynamics with a high-visibility canopy or estimating the longitudinal aerodynamic characteristics of configurations with highly noncircular cross sections are addressed. Also included is a discussion of the efficiency of conducting analyses such as these on a computer system which is substantially less sophisticated than state-of-the-art supercomputers, but which is widely available in government and industry facilities.

Discussion

The ultimate purpose of any aerodynamic design or analysis technique - whether it be a sophisticated computational fluid dynamics algorithm or a relatively simple linear theory approach - is to provide accurate and timely answers to practical engineering problems. The aerodynamic design and analysis environment requires that a large number of calculations be made as a new design is sized and optimized, and thus the tools employed must be efficient and easily adaptable to changing configuration geometries and flight envelope requirements. The configuration modeling process must allow convenient and rapid geometry variations as the design is refined. The selected code should be robust and not require an unusually high level of user expertise to achieve timely and accurate results.

Methodology

The full potential methodology selected for the analyses presented in this paper is rapidly maturing to a level which meets the design and analysis tool characteristics described above. The method has been described in detail in a number of papers[8,9,10,11,12] and thus will only be summarized here.

The numerical method solves the full potential equation in conservation form for the supersonic flow past arbitrary and complex geometries. Configurations which can be treated may include a fuselage, canopy, wing, canard, nacelle, vertical and horizontal tails, and inlets. A flux linearized upwind differencing technique is employed to advance the solution along the configuration. The finite difference equations are solved using an implicit factorization scheme. Embedded subsonic regions are treated using conservative switching operators to transition from the supersonic marching algorithm to a subsonic relaxation technique. Computational grids between the body surface and a user specified outer boundary are developed using an elliptic grid generation routine. Boundary conditions require no net normal flow at the body surface and freestream conditions at the outer boundary which is set outside the bow shock location. A starting data plane is established near the nose of the configuration to initiate the solution. For sharp-nosed configurations conical starting solutions are generated while for blunt noses a method based on the axisymmetric unsteady full potential equation[13] is employed.

The geometry modeling requirements of this method are particularly attractive. Analytical descriptions of the configuration are not required. Instead, a surface description of a number of configuration cross sections is specified on a point-by-point basis. This type of geometry information is readily obtainable during the early stages of a configuration design and allows for efficient updates to the numerical model as the configuration is modified and refined. The cross section defining points are splined by the code to obtain complete cross section definitions while linear interpolation is employed in the streamwise direction for marching

plane locations between the input stations.

This full potential method solves the entire flow field between the body surface and the outer boundary. Program output consists of velocity components and pressure coefficients at all grid points and overall force and moment components on the configuration.

Fighter Forebody Analysis

A fighter forebody with and without canopy for which experimental pressure and force data were available[14] was selected for analysis. Figure 1 illustrates the geometric details of the configuration with the canopy. Wireframe representations of the forebody alone and with the canopy in place are shown in Figure 2. Test data were available for these two configurations at Mach numbers of 1.41 and 2.01 for angles of attack ranging from -6^{o} to $+12^{o}$. Although test results for nonzero sideslip angles are also available, only the zero sideslip cases were considered in the present analysis.

As noted in Figure 1, both the forebody and canopy cross-section shapes are ellipses and thus the surface point definitions of the defining cross sections were easily and conveniently obtained from the equations for the ellipses. The line of intersection between the canopy and forebody (i.e., the parting line) was similarly determined.

A computational grid containing 20 points in the normal direction and 30 points in the circumferential direction (a 20x30 grid) was specified for the full potential code analyses. Typical grids for both configurations are shown in Figure 3. Marching solutions for the forebody alone were obtained in a single program run, while three runs were required for the forebody with canopy - one for the forebody forward of the canopy, one for the canopy region, and one for the aft-body. In each case, the marching step size was determined internally by the code based on CFL number considerations.

Computed pressure distributions along the forebody top centerline at Mach 2.01 for angles of attack of 0.4^{o}, 6^{o}, and 12^{o} are presented in Figure 4. The full potential code results agree well with the data and accurately predict the variation in pressures associated with the angle of attack changes. Some irregularity in the computed pressure coefficients occurs near the nose, however, and at 12^{o} angle of attack there is a lack of agreement with the test data over the rearward portion of the forebody where pressure values are more positive than the measured data.

Similar results are shown in Figure 5 for a Mach number of 1.41 and angles of attack of 0.4^{o}, 3^{o}, and 9^{o}. The full potential results agree quite well with the test data at $\alpha = 0.4^{o}$ and 3^{o}. Accurate results were not obtained for the rear half of the forebody at the 9^{o} angle of attack, however. For this case, the 20x30 grid was modified to a 30x30 grid to increase the normal grid density in an attempt to improve the computed results. As shown in Figure 5, however, these results with the increased grid density are essentially the same as for the original 20x30 grid. At this combination of low Mach number and relatively high angle of attack, the code is apparently unable to properly handle the adverse pressure gradient along the lee side (top centerline) of the forebody. Decreasing the marching step size might improve the numerical results in this case.

As shown in Figure 5, oscillations in the full potential code pressure distributions occur near the nose of the forebody. The reasons for these oscillations were, at present, not determined although they may be related to the transition from the conical starting solution to the nonconical marching technique. They do not appear to be related to a possible error in the input geometry as they occur at different longitudinal locations for the angles of attack considered. As will be shown, these oscillations have little effect on the computed force coefficients.

Comparisons of the measured pressure coefficients and the full potential code results for the forebody with canopy are shown in Figure 6. Pressure coefficients along the canopy-forebody parting line (line of intersection) are plotted against canopy fractional length for angles of attack of 0^{o}, 6^{o}, and 12^{o} at Mach 2.01. In general, the full potential code results agree very well with the measured data. At 12^{o} angle of attack, however, there is a sizable region over the forward twenty-five percent of the canopy where poor agreement between the computed and measured pressure coefficients occurs. This lack of agreement is

most likely due to a pocket of subsonic flow. A more detailed calculation for the subsonic pocket would probably improve these results. Also note that some oscillation occurs in the computed pressure distributions as has been described for the forebody alone.

Figures 7 and 8 summarize lift and drag coefficient results for the forebody alone. Similar results with the canopy are presented in figure 9. The full potential lift results agree very well with the measured data and accurately reflect the nonlinear characteristics. The drag correlation includes an estimate of the skin friction obtained using the T' method[15]. The full potential drag plus skin friction results agree reasonably well with the measured data for the forebody alone at Mach 1.41 but uniformly underpredict the drag at Mach 2.01 for both configurations. This underprediction appears to be related to the skin friction estimate. Note in particular that oscillations in the computed pressure distributions and local areas of disagreement between the measured and predicted pressures did not result in significant errors in the computed force coefficients.

Supersonic Cruise Configuration Analysis

Figure 10 illustrates a supersonic cruise configuration for which a set of both pressure data and force and moment data are available[16,17]. This Mach 3.0 design employs a modified arrow wing planform with a leading-edge sweep of 75° inboard and 60° in the wing tip region. A chine extends aft from the fuselage nose and blends into the wing leading edge at the wing side-of-body location. A minimum drag wing twist and camber distribution is employed for improved supersonic performance. Other configuration components include flow-through nacelles located at the 31 percent wing semispan location, twin vertical tails mounted atop the wing where the leading-edge sweep changes from 75° to 60°, and a ventral fin mounted on the aircraft plane of symmetry.

The model geometry was measured on a three-axis dimension-recording machine to obtain accurate details of the model as tested. These measured geometric values were used to develop the numerical models for the full potential code analysis presented herein.

The full potential code has been used to analyze the wing-body combination at a Mach number of 2.3 and angles of attack of -0.18°, 5.81°, and 11.82°. Both pressure coefficient and force/moment coefficient correlations between the predicted and measured data have been made.

Typical computational grids for the cruise configuration are illustrated in Figure 11. Grid densities ranged from 25x29 to 32x61 as the solution progressed down the length of the configuration. Gridding was specified in two regions with the dividing line being the normal grid line which emerges from the wing tip.

Comparisons of the computed and measured surface pressure distributions for the wing-body at Mach 2.3 for angles of attack of 5.80° and 11.82° are shown in Figures 12 and 13. The cross section locations selected for these comparisons correspond to those previously shown in Figure 10.

At α = 5.81°, the comparison between the predicted and measured results is excellent at station 25.53, but only fair at station 35.10. Although the lower surface pressures are well predicted at the more aft station, the upper surface values are more negative than the test data near the wing leading edge.

The agreement for α = 11.82° is good to fair. At station 25.53, the predicted upper surface pressures are again too negative while at station 35.10, the lower surface values are less positive than the measured data. The reasons for the lack of agreement between the predicted and measured pressures is presumed to be related to the inability of the full potential method to model the vortex flows generated by the chine and highly-swept wing leading edge. This vortex flow intensifies as the angle of attack increases, and the more aft longitudinal stations see a more fully developed vortex than do the forward stations.

The near-constant upper surface pressures shown in Figure 13 for the outer portion of the wing reflect the pressure limiting incorporated into the full potential code. This feature prevents the computed pressures from exceeding the isentropic vacuum limit, $-2/\gamma M_\infty^2$. Pressure limiting is implemented through the density term in the full

potential equation solution. This approach prevents numerical errors which result from negative density values developed near the wing leading edge where the flow expands from the lower to the upper surface.

As will subsequently be shown, these discrepancies in pressure coefficient result in relatively minor errors in the computed force coefficients.

Figure 14 illustrates the computational grid and pressure coefficient profile at station 47.56 where the wing wake is present along with the outboard wing panel. The angle of attack is 5.81°. The representation of wakes in the full potential code is done in an approximate manner. The full potential equation is not solved at wake points. Instead the equation $\Phi_{\eta\eta} = 0$ is solved such that the pressure change across the wake is approximately zero. The wake is thus a transparent surface through which flow may pass. As Figure 14 shows, realistic wake characteristics can be obtained using this approach.

Lift results for the supersonic cruise wing-body configuration are presented in Figure 15 for a Mach number of 2.3. The agreement between the predicted and measured data is excellent for the lift.

The T' method was used to estimate a skin friction increment for the configuration. This result was combined with the pressure drag obtained from the full potential code to obtain the drag polar shown in Figure 15. The agreement with the test data is excellent for lift coefficients up to about 0.15. Above this value, the agreement is good, although the drag is slightly underpredicted.

Nonlinear pitching moment characteristics are particularly difficult to accurately estimate-especially at the higher angles of attack. As shown in Figure 16, the full potential method very nicely predicts the trend of pitching moment with increasing lift coefficient, but somewhat fails to accurately estimate the magnitude. Errors in the computed pressures are evident in this case even though compensating errors probably contributed to some extent to the quality of the lift and drag predictions.

Overall, the full potential code has provided accurate estimates of both the aerodynamic loading and the longitudinal aerodynamic characteristics of the configuration.

Computer Hardware Considerations

Table I summarizes typical VAX 11/780 execution times for the configurations analyzed. Note that all analyses were conducted using single-precision (32-bit) arithmetic. Also, the VAX 11/780 computer system utilized has a floating-point accelerator.

TABLE I. VAX 11/780 EXECUTION TIMES

Configuration	CPU Time (Hours:Minutes)
Forebody Alone	0:27
Forebody + Canopy	0:45
Supersonic Cruise Wing-Body	4 :11

NOTE: Single-precision arithmetic in all cases.

The VAX 11/780 is a relatively slow machine when compared to more sophisticated hardware, but the execution times shown in Table I are considered to be reasonable and acceptable. Computers of the type used in these analyses are widely available in government and industry and are relatively inexpensive to purchase and operate. The total cost per analysis is thus low.

The full potential code used in these analyses was originally developed for the Control Data Corporation Cyber 173, 175 machines. Conversion to the VAX 11/780 was very straightforward, but no attempt was made to optimize the code for the VAX environment. Additional work in this area would certainly result in a more efficient code for the VAX with corresponding reductions in execution times.

The VAX 11/780 is a virtual memory machine. This feature allows higher computational grid densities to be used when necessary by simply revising the FORTRAN DIMENSION statements and re-compiling the code. Fixed memory machines such as the Cybers are limited to a maximum grid size which may not be adequate in all cases.

Figure 17 illustrates the relative accuracy of single-precision versus double-precision arithmetic in executing

the full potential code. The configuration selected for this analysis was the forebody alone at Mach 2.01 and 0.4° angle of attack. The computational grid in each case was 20x30. As the pressure distributions in the figure show, essentially identical numerical results were obtained in both cases. The double-precision case, however, required nearly twice the execution time. No code problems due to numerical precision were encountered in using the single-precision arithmetic.

Summary

A method based on the conservation form of the full potential equation has been used to analyze realistic aircraft configurations at supersonic speeds. A fighter forebody with and without a canopy and a supersonic cruise wing-body configuration have been addressed in the Mach 1.41 to 2.3 speed range.

Predicted and measured surface pressures for the forebody agreed very well for angles of attack from 0° to 12°. Although oscillations in the computed pressure distributions were noted in some cases, the force coefficient correlations were good to excellent.

Good to excellent pressure distribution comparisons with wind tunnel data for the supersonic cruise wing-body configuration were obtained as well. The overall lift and drag estimates were in excellent agreement with the test data. The nonlinear character of the pitching moment variation with lift coefficient was well predicted by the full potential code although the estimated magnitudes were somewhat lower.

These analyses were conducted using single-precision arithmetic on a VAX 11/780 computer system. No numerical problems were evident in using the 32-bit arithmetic, and the execution times were considerably faster than when using double precision. Forebody solutions required about one-half to three-quarters of an hour of central processor time while the wing-body runs averaged slightly over four hours. These times are considered reasonable and acceptable for a widely available computer system which is reasonably inexpensive to obtain and operate. Reduction in execution times are anticipated through optimization of the FORTRAN code for the VAX environment.

The full potential code represents a useful and economical bridge between the linear theory and Euler methods. Further application and improvement of the method will result in a reliable design and analysis tool which can be confidently applied to a variety of supersonic problems.

References

1. Middleton, W.D. and Lundry, J.L.: A System for Aerodynamic Design and Analysis of Supersonic Aircraft. Part 1- General Description and Theoretical Development. NASA CR 3351, 1980.

2. Baals, D.D.; Robins, A.W.; and Harris, R.V., Jr.: Aerodynamic Design Integration of Supersonic Aircraft. AIAA Paper 68-1018, 1968.

3. Walkley, K.B. and Martin, G.L.: Aerodynamic Design and Analysis of the AST-200 Supersonic Transport Configuration Concept. NASA CR 159051, 1979.

4. Rizk, Y.M. and Ben-Shmuel, B.: Computation of the Viscous Flow Around the Shuttle Orbiter at Low Supersonic Speeds. AIAA Paper AIAA-85-0168, 1985.

5. Moitra, A.: Numerical Solution of the Euler Equations for High-Speed, Blended Wing-Body Configurations. AIAA Paper AIAA-85-0123, 1985.

6. Chakravarthy, S.R. and Szema, K.Y.: An Euler Solver for Three-Dimensional Supersonic Flows with Subsonic Pockets. AIAA Paper AIAA-85-1703, 1985.

7. Ross, J.M.; Reaser, J.S.; and Bouchard, E.E.: Optimization of a Supersonic Wing by Combining Linear and Euler Methods. SAE Paper 851791, 1985.

8. Shankar, V.; Szema, K.Y.; and Bonner, E.: Full Potential Methods for Analysis/Design of Complex Aerospace Configurations. NASA CR 3982, 1986.

9. Shankar, V.: Conservative Full Potential, Implicit Marching Scheme for Supersonic Flows. AIAA Jour., Vol. 20, No. 11, November 1982.

10. Shankar, V. and Osher, S.: An

Efficient Full-Potential Implicit Method Based on Characteristics for Supersonic Flows. AIAA Jour., Vol. 21, No. 9, September 1983.

11. Shankar, V.; Szema, K.Y.; and Osher, S.: Treatment of Supersonic Flows with Embedded Subsonic Regions. AIAA Jour., Vol. 23, No. 1, January 1985.

12. Szema, K.Y.; Riba, W.L.; Shankar, V.; and Gorski, J.J.: Computation of Supersonic Flows over Three-Dimensional Configurations. Jour. of Aircraft, Vol. 22., No. 12, December 1985.

13. Shankar, V.; Ide, H.; and Gorski, J.: Relaxation and Approximate Factorization Methods for the Unsteady Full Potential Equation. 14th Congress of the International Council of the Aeronautical Sciences, September 9-14, 1984, Toulouse, France. Paper No. ICAS-84-1.6.2.

14. Robins, A.W.: Force and Pressure Measurements on Several Canopy-Fuselage Configurations at Mach Numbers 1.41 and 2.01. NACA RM L55H23, 1955.

15. Sommer, Simon C. and Short, Barbara J.: Free-Flight Measurements of Turbulent-Boundary-Layer Skin Friction in the Presence of Severe Aerodynamic Heating at Mach Numbers from 2.8 to 7.0. NACA TN 3391, 1955.

16. Shrout, B.L. and Fournier, R.H.: Aerodynamic Characteristics of a Supersonic Cruise Airplane Configuration at Mach Numbers of 2.30, 2.96, and 3.30. NASA TM 78792, 1979.

17. Shrout, B.L.; Corlett, W.A.; and Collins, I.K.: Surface Pressure Data for a Supersonic-Cruise Airplane Configuration at Mach Numbers of 2.30, 2.96, and 3.30. NASA TM 80061, 1979.

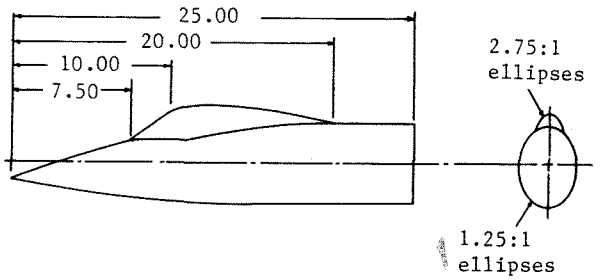

Figure 1. Forebody configuration. All linear dimensions are in inches.

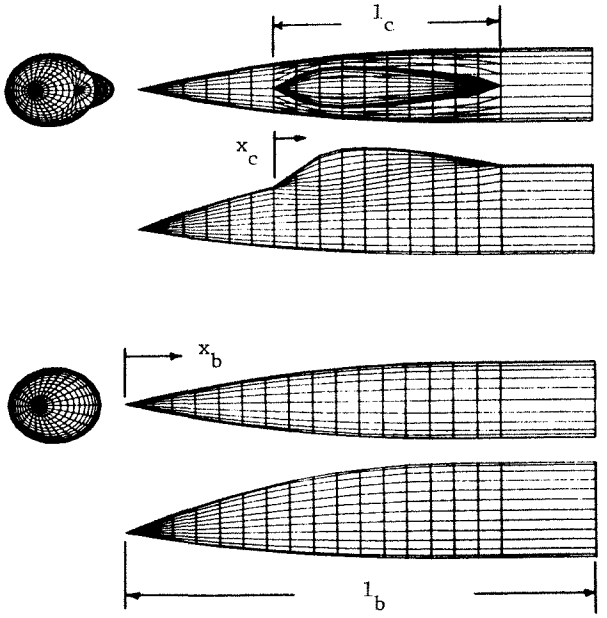

Figure 2. Forebody wireframe representations with and without the canopy.

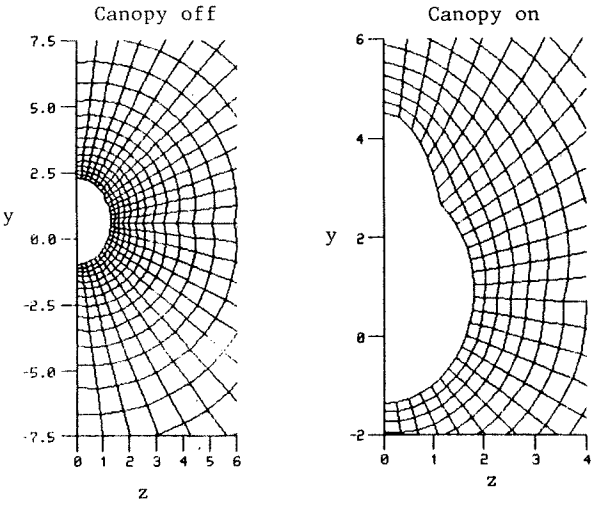

Figure 3. Typical computational grids for the forebody.

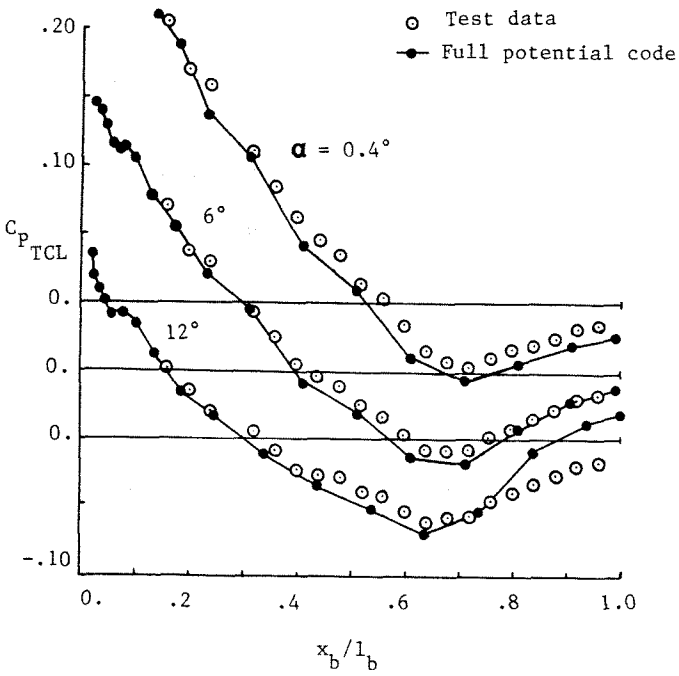

Figure 4. Comparison of full potential code results and test data for the forebody alone at Mach 2.01

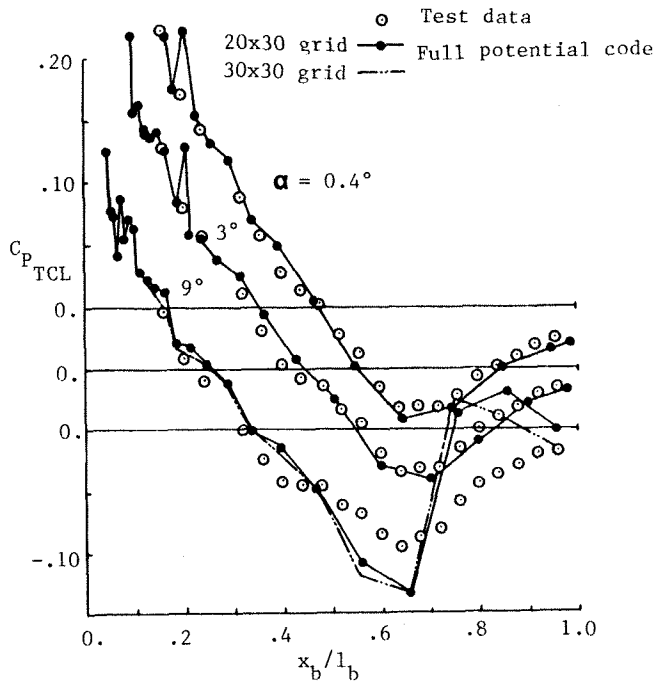

Figure 5. Comparison of full potential code results and test data for the forebody alone at Mach 1.41.

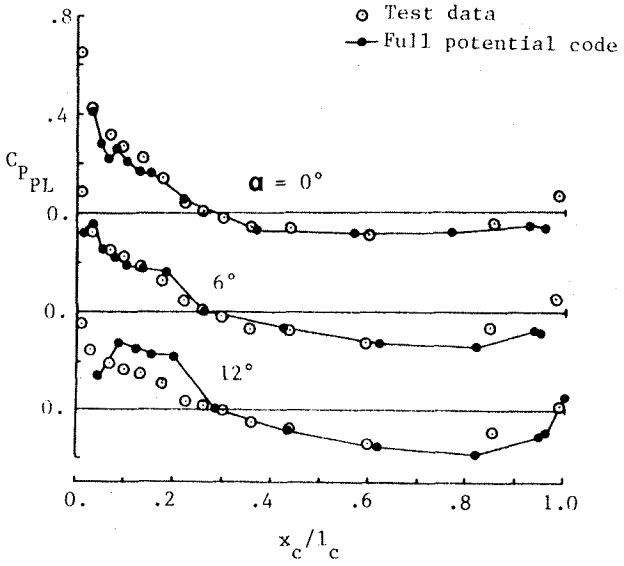

Figure 6. Comparison of canopy-forebody parting-line pressures at Mach 2.01.

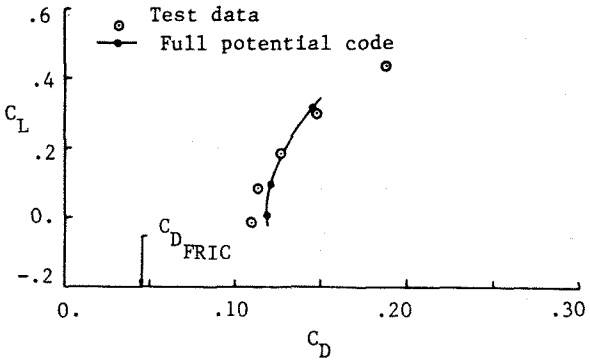

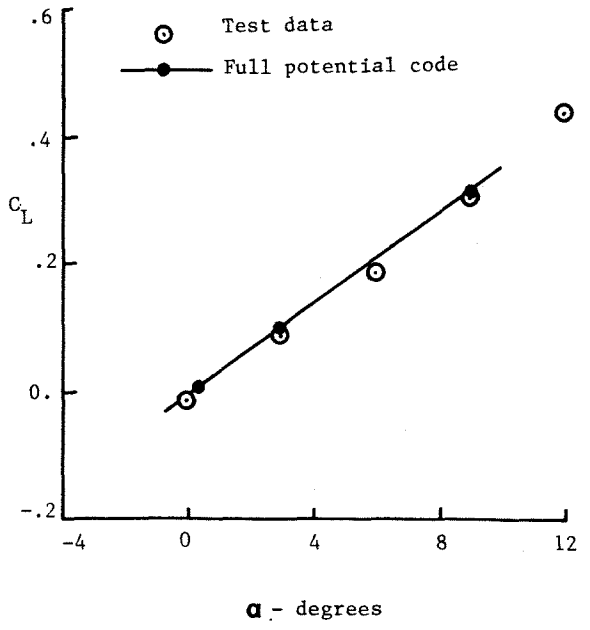

Figure 7. Lift and drag results for the forebody alone at Mach 1.41.

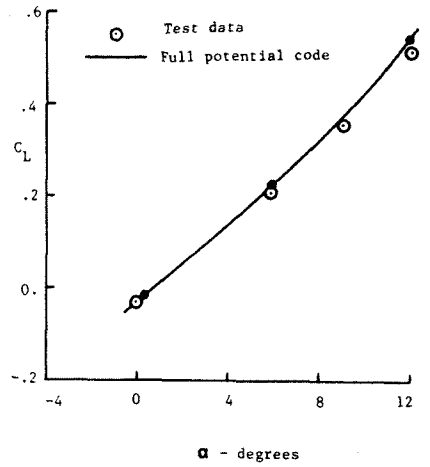

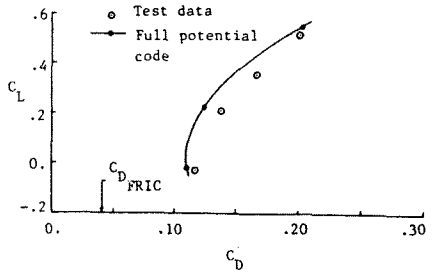

Figure 8. Lift and drag results for the forebody alone at Mach 2.01.

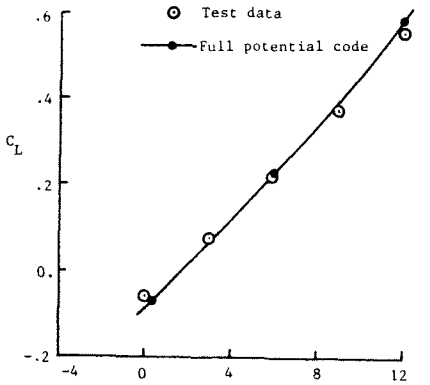

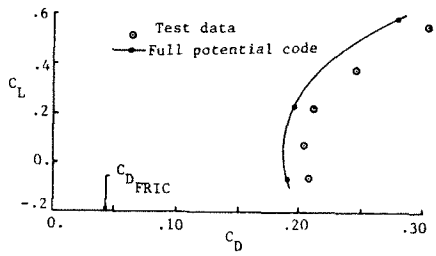

Figure 9. Lift and drag results for the forebody and canopy at Mach 2.01.

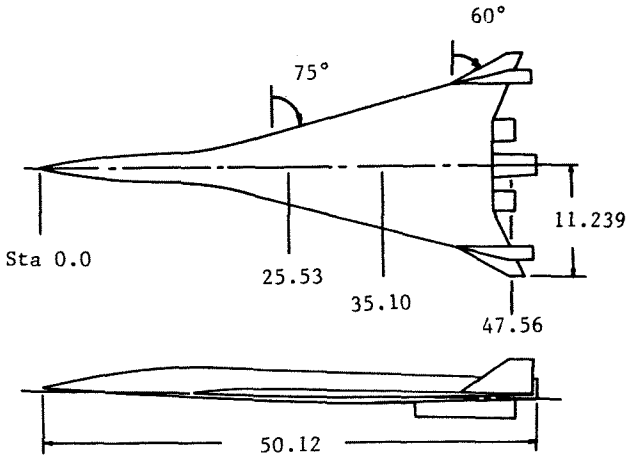

Figure 10. Supersonic cruise configuration. All linear dimensions are in inches.

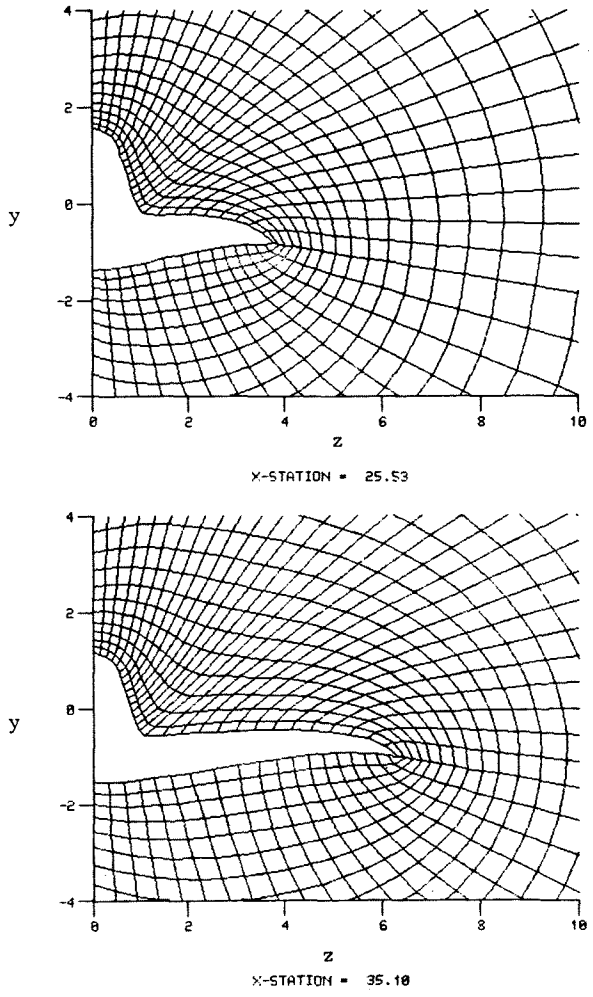

Figure 11. Typical computational grids for the wing-body configuration.

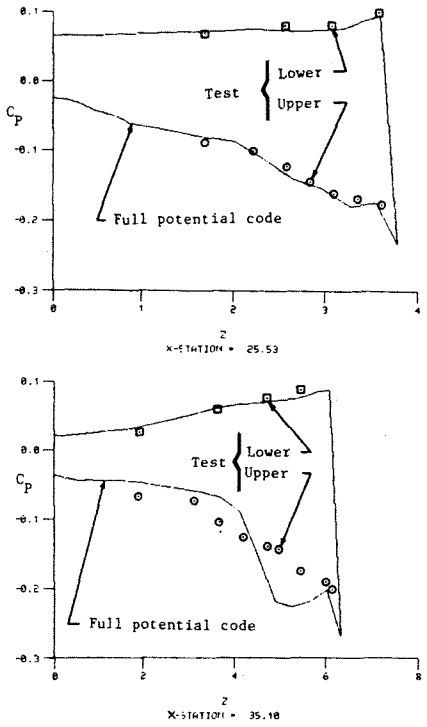

Figure 12. Pressure coefficient profiles for the wing-body configuration at $\alpha = 5.81^{\circ}$.

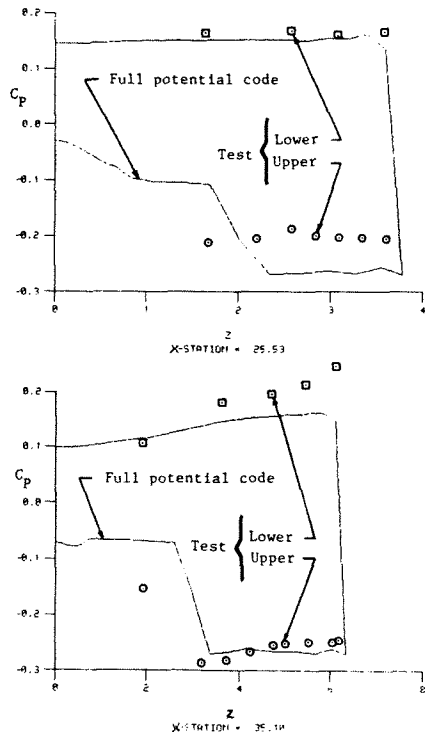

Figure 13. Pressure coefficient profiles for the wing-body configuration at $\alpha = 11.82^{\circ}$.

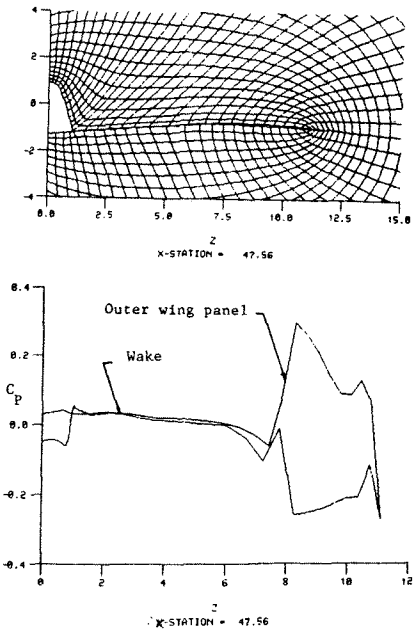

Figure 14. Wake results.

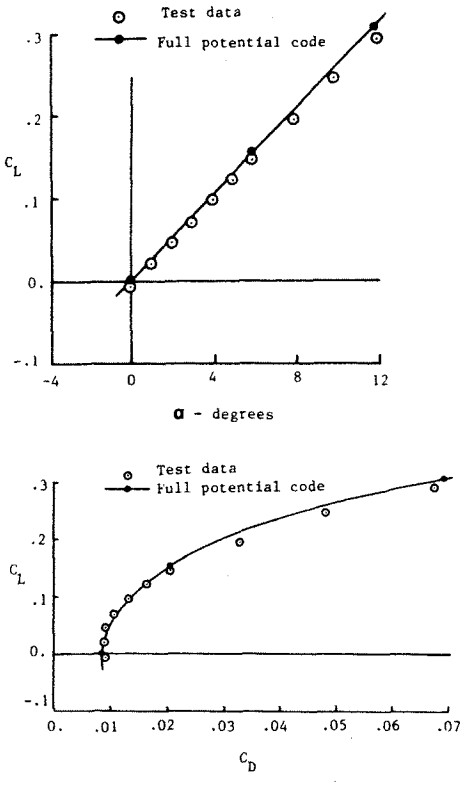

Figure 15. Lift and drag coefficients for the wing-body configuration at Mach 2.30.

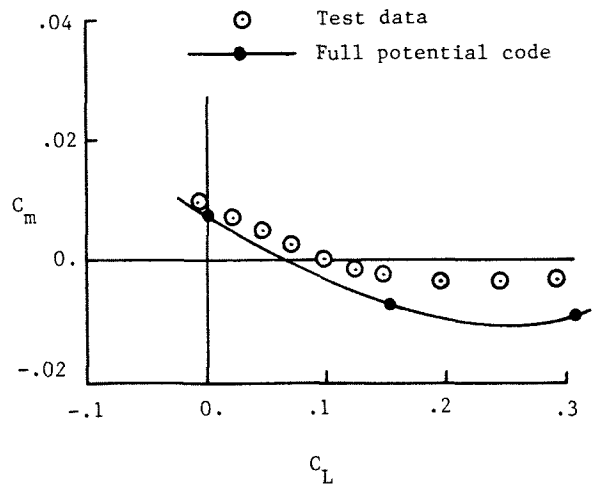

Figure 16. Pitching moment coefficients for the wing-body configuration at Mach 2.30.

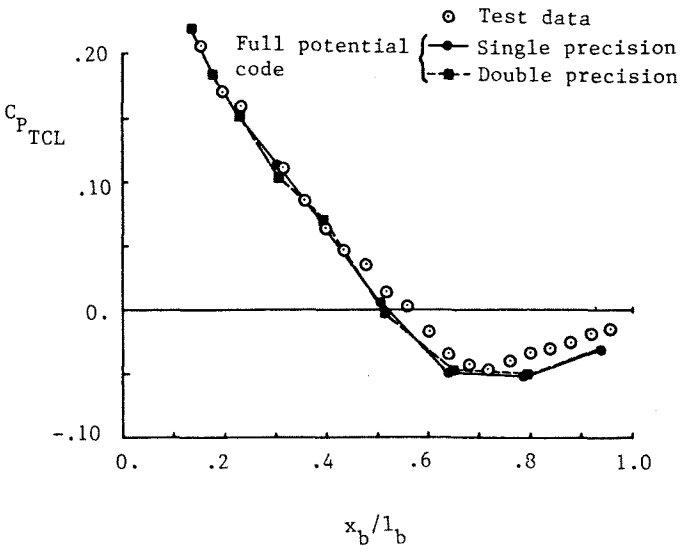

Figure 17. Single- and double-precision full potential code results for the forebody alone. Mach 2.01, $\alpha = 0.4^{\circ}$